Supplementary Material

Deterpenation of *citrus* essential oils via extractive distillation using imidazolium-based ionic liquids as entrainers

Sérgio M. Vilas-Boas[a,b,c,d], Fábio R. M. Batista[e], Rafael M. Dias[f], João A. P. Coutinho[c], Olga Ferreira[a,b], Mariana C. da Costa[d*], Simão P. Pinho[a,b*]

[a]Centro de Investigação de Montanha (CIMO), Instituto Politécnico de Bragança, Campus de Santa Apolónia, 5300-253 Bragança, Portugal

[b]Laboratório para a Sustentabilidade e Tecnologia em Regiões de Montanha, Instituto Politécnico de Bragança, Campus de Santa Apolónia, 5300-253 Bragança, Portugal

[c]CICECO − Aveiro Institute of Materials, Department of Chemistry, University of Aveiro, 3810-193 Aveiro, Portugal.

[d]School of Chemical Engineering (FEQ), University of Campinas (UNICAMP), 13083-852 Campinas, Brazil

[e]Department of Chemical Engineering, School of Engineering of Lorena, University of São Paulo - USP, Lorena, 12602-810, SP, Brazil

[f]Chemical Institute (IQ), Federal University of Goiás – UFG, Campus Samambaia, 74001-970, Goiânia, GO, Brazil

***Corresponding authors:**

Mariana C. da Costa, Phone: + 55 1935213962, E-mail: mcdcosta@unicamp.br

Simão P. Pinho, Phone: +351 273303086, E-mail: spinho@ipb.pt;

Section S1. Complementary information for Process simulation

Process simulation in the Aspen Plus software

The ILs were introduced as User-Defined components in the Aspen Plus software. More details on the calculation procedures of IL heat capacities, enthalpies of vaporization, and vapor pressure are presented in Section S2, and the parameters imputed in Aspen are listed in Table S1. For limonene and linalool, the required thermophysical properties were directly collected from the property databank of Aspen Plus. The NRTL model [1,2] was used to represent the VLE data of the limonene/linalool and limonene/linalool/IL mixtures, and the vapor phase was considered ideal.

The rigorous two-phase fractionation (RADFRAC model) was selected to simulate the extractive distillation column, operating at 5 kPa. The model CEO feed flow of the distillation column (F) was set to 1000 kg·h^{-1}, at 298.2 K and 101.3 kPa. The two-outlet (FLASH2 model) was selected to represent the flash unit. Since the essential oils are susceptible to degradation when exposed to high temperatures [3], the flash unit was operating at 363.2 K. Preliminary tests in Aspen Plus showed that a pressure of 100 Pa in the flash unit delivers good recoveries of the terpeneless CEO when [C$_4$mim]Cl is used as the entrainer, while for [C$_4$mim][OAc], the $^{\text{pressure}}$ was set at 5 Pa.

Prediction of the CO_2 emissions

The CO_2 emission is an important parameter for tracking the environmental performance of distillation-based processes [4]. Besides, this parameter is strongly related to the energy consumption of a distillation column since most of its required reboiler and heat exchange network is directly or indirectly related to the combustion of fossil fuels [5]. Therefore, the CO_2 emissions are modeled in this work considering the approach proposed by Gadalla et al. [6] and applied in several distillation-based separation processes [4,5,7–9]. Assuming that complete combustion occurs (i.e., air is in excess and no carbon monoxide is formed), the CO_2 emissions (kg·h^{-1}) can be calculated by the as following: [6]

$$[\mathrm{CO_2}]_{\mathrm{Emiss}} = \left(\frac{Q_{Fuel}}{NHV}\right)\left(\frac{C\%}{100}\right)\alpha \qquad \textbf{(1)}$$

where Q_{Fuel} is the heat released from the fuel combustion, NHV is the net calorific value of the fuel with a carbon content of $C\%$ (i.e., heavy fuel oil with $C\% = 86.5\%$ and $NHV =$

51600 kJ·kmol^{-1} are considered in this work [6]), and α is the molar masses ratio of CO_2 and C_{12} (α = 3.67). When no heated integration is considered in a distillation-based separation process, the energy provided from the fuel burnt to the steam boiler of the distillation column can be calculated as [4,6]:

$$Q_{Fuel} = \frac{Q_{proc}}{\lambda_{proc}}\left(h_{proc} - 419\right)\left(\frac{T_{FTB} - T_0}{T_{FTB} - T_{stack}}\right) \quad \textbf{(2)}$$

where Q_{proc} is the reboiler heat duty, λ_{proc} (kJ·kg^{-1}) and h_{proc} (kJ·kg^{-1}) are the latent heat and enthalpy of the steam delivered to the process, respectively. In addition, T_{FTB}, T_{stack} and T_0 are the flame, stack and room temperatures, respectively (i.e., the values used in this work are $T_{FTB} = 1800$ ºC, $T_{stack} = 160$ ºC, and $T_0 = 25$ ºC [6]). The boiler feedwater is assumed to be at 100 ºC, with an enthalpy of 419 kJ·kg^{-1}[6].

Section S2. Calculation of the Ionic Liquid required properties to be introduced in Aspen Plus

Vapor pressures

No vapor pressure data were found in the literature for [C4mim][OAc] and [C4mim]Cl. Therefore, the predictive method proposed by Hekayati et al. [10] was applied. In this method, the vapor pressure of an ionic liquid (IL) is related to its critical properties as follows:

$$\ln P^{sat} = f^{(0)} + \omega \times f^{(1)} \quad \textbf{(3)}$$

$$f^{(0)} = A - \frac{B}{T} - C \times T \times \frac{Z_C}{T_C} + D \times V_C \times n\left(C_{R_2}\right) - E \times {V_C}^2 - F \times n\left(C_{R_2}\right)^2 \quad \textbf{(4)}$$

$$f^{(1)} = G - \frac{H}{T} \quad \textbf{(5)}$$

where P^{sat} is the estimated vapor pressure (bar) at temperature T (K), ω is the acentric factor, $n\left(C_{R_2}\right)$ is the number of carbons of the second alkyl group of the IL cation, Z_C, T_C, V_C correspond to the critical compressibility factor, the critical temperature (K), and the critical volume ($cm^3 \cdot mol^{-1}$), respectively, and A, B, C, D, E, F, G, and H are estimated parameters that are applicable for all ILs and are reported by Hekayati et al. [10]. The IL critical properties were retrieved from the database reported by Valderrama et al. [11]

Ideal-gas heat capacities

The ideal-gas heat capacities (${C_p}^{\circ}$) of the ILs were correlated to the available heat capacity data of the liquid phase (C_p) [12,13] using the following relation: [14]

$$\frac{C_p - {C_p}^{\circ}}{R} = 1.586 + \frac{0.49}{1 - T_r} + \omega \times \left[4.2775 + \frac{6.3 \times (1 - T_r)^{1/3}}{T_r} + \frac{0.4355}{1 - T_r}\right] \quad \textbf{(6)}$$

where R is the gas constant (8.31447 $J \cdot mol^{-1} \cdot K^{-1}$ [15]) and T_r is the reduced temperature.

Enthalpies of vaporization

The temperature-dependent enthalpies of vaporization ($\Delta H_{Vap,T}$) of the studied ILs were predicted using the approach recently proposed by Verevkin et al. [16]:

$$\Delta H_{Vap,T} = \Delta_l^g C_p \times (T - 298.15) - \Delta H_{Vap,298.15} \quad \textbf{(7)}$$

$$\Delta_l^g C_p = -0.126 \times C_p - 1.5 \quad \textbf{(8)}$$

where $\Delta H_{Vap,298.15}$ is the enthalpy of vaporization of the IL at 298.15 K and $\Delta_l^g C_p$ is the difference between the heat capacity of gaseous and liquid phases. In this approach, $\Delta_l^g C_p$ values are derived using the empirical relation presented in Eq. **(8)** [16].

Table S1. List of parameters of the ionic liquids [C_4mim][OAc] and [C_4mim]Cl introduced as User-Defined compounds in Aspen Plus.

Parameter	**Ionic liquids**[a]	
	[C_4mim][OAc]	**[C_4mim]Cl**
Molar mass (g·mol^{-1})	198.262 [17,18]	174.671[17,18]
$\boldsymbol{\Delta H_{Vap,298.15}}$ (kJ·mol^{-1})	134.8 [19]	153.5 [20]
Critical properties		
$\boldsymbol{T_C}$ (K)	847.3 [11]	789.0 [11]
$\boldsymbol{V_C}$ (cm^3·mol^{-1})	658.2 [11]	568.8 [11]
$\boldsymbol{P_C}$ (bar)	24.5 [11]	27.8 [11]
$\boldsymbol{Z_C}$ (K)	0.229 [11]	0.241 [11]
$\boldsymbol{\omega}$	0.668 [11]	0.491 [11]
Vapor pressure constants[b]		
$\boldsymbol{C_1}$ (Pa)	8.93	7.10
$\boldsymbol{C_2}$ (K·Pa)	4130.8	3555.7
$\boldsymbol{C_3}$ (K)	-78.16	-93.05
Ideal heat capacity constants[c]		
$\boldsymbol{C_1}$ (J·kmol^{-1}·K^{-1})	38992.96	423279.52
$\boldsymbol{C_2}$ (J·kmol^{-1}·K^{-2})	1435.02	-2444.50
$\boldsymbol{C_3}$ (J·kmol^{-1}·K^{-3})	-1.912	8.056
$\boldsymbol{C_4}$ (J·kmol^{-1}·K^{-4})	0.0013	-0.0072
Enthalpy of vaporization constats[d]		
$\boldsymbol{C_1}$ (J·kmol^{-1})	18.79	18.83
$\boldsymbol{C_2}$ (J·kmol^{-1})	0.068	-0.284
$\boldsymbol{C_3}$ (J·kmol^{-1})	0.350	0.882
$\boldsymbol{C_4}$ (J·kmol^{-1})	-0.231	-0.558

[a]References are listed after the values.

[b]Vapor pressures were fitted to the LOGVP1 Aspen plus equation format: $\log(P^{sat}) = C_1 + \frac{C_2}{T + C_3}$; P^{sat}/Pa and T/K.

[c]Ideal-gas heat capacities were fitted to the CPIG Aspen plus equation format: $C_p{}^{o} = C_1 + C_2 \times T + C_3 \times T^2 + C_4 \times T^3$; $C_p{}^{o}$/J·kmol^{-1}·K^{-1} and T/K.

[d]Enthalpies of vaporization were fitted to the DHVLTDEW Aspen plus equation format: $\ln(\Delta H_{Vap,T}) = C_1 + C_2 \times \ln(1 - T_r) + C_3 \times T_r \times \ln(1 - T_r) + C_4 \times T_r{}^2 \times \ln(1 - T_r)$; $\Delta H_{Vap,T}$/J·kmol^{-1} and T/K.

Section S3. Validation of the apparatus for the VLE measurements

Assessment of the deviations

The deviations between the experimental and correlated data were assessed by calculating the root-mean-square deviations (σ):

$$\sigma = \sqrt{\left[\frac{\sum_i \left(M_i^{exp} - M_i^{calc}\right)^2}{n}\right]} \quad \textbf{(9)}$$

where M is the evaluated property, n is the total number of data points, and the subscripts *exp* and *calc* correspond to the experimental and calculated data, respectively.

Vapor pressure measurements

The vapor pressures of pure ethanol and R-(+)-limonene measured in this work are compared with the literature data in **Figure S1** and listed in **Table S2**. The ln(p) vs 1/T plot reveals good consistency of the experimental data obtained in this work for both compounds ($R^2 > 0.99985$). To further assess the data's reliability, the vapor pressures obtained in this work for ethanol were compared to the values calculated with Antoine Equation parameters evaluated by NIST [21,22]; a low σ value of 1.2 kPa was obtained. Nevertheless, the Antoine parameters are unavailable in the NIST database for R-(+)-limonene. Thus, for this compound, Antoine parameters regressed with vapor pressure data available in the literature [23–28] were used to calculate the vapor pressures in the temperature range measured in this work, resulting in a σ value of 2.4 kPa. The Antoine parameters fitted with the experimental data obtained in this work are presented in **Table S3**.

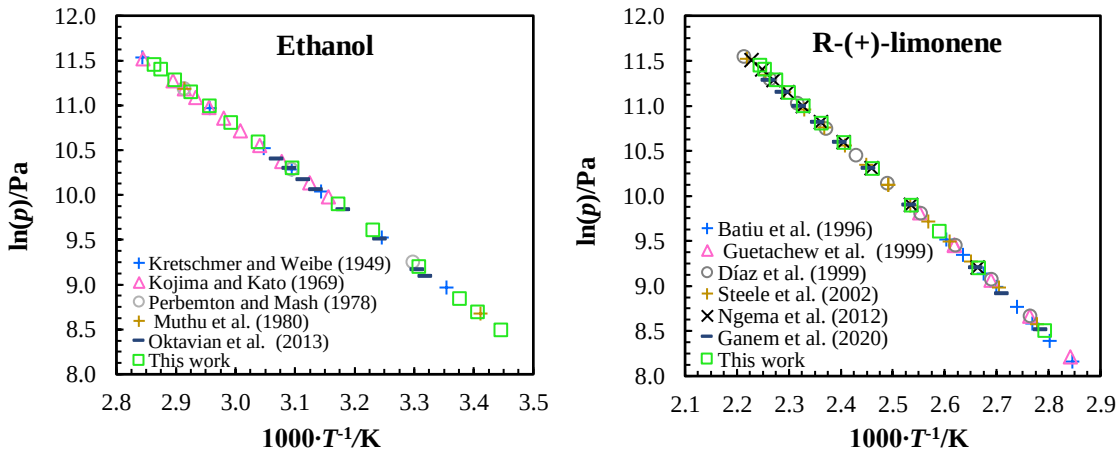

Figure S1. Comparison of the vapor pressures measured in this work with the literature data for ethanol [29–34] and R(+)-limonene [23–28].

Table S2. Experimental vapor pressures of ethanol and R-(+)-limonene measured in this work[a]

ethanol		R-(+)-limonene	
***T*/K**	***p*/kPa**	***T*/K**	***p*/kPa**
290.2	4.9	358.1	5.0
293.6	6.0	375.1	9.9
296.2	7.0	386.1	14.9
302.3	9.9	394.3	19.9
309.5	14.9	406.4	29.8
315.2	19.9	415.6	39.8
323.1	29.8	423.3	49.6
329.2	39.8	429.5	59.7
334.2	49.7	434.8	69.7
338.3	59.6	439.5	79.8
341.9	69.5	443.9	89.7
345.0	79.4	445.5	94.3
347.9	89.7		
349.2	94.7		

[a]Temperature and pressure standard uncertainties are $u(T)$ = 0.1 K and $u(p)$ = 0.1 kPa, respectively

Table S3. Antoine coefficients (*A*, *B*, and *C*) regressed with the experimental vapor pressures measured in this work and the data retrieved from the literature.[a]

Compound	***A***	***B***	***C***
Ethanol	10.306	1614.313	-46.310
R-(+)-limonene	9.774	2001.397	-28.741

[a]The vapor pressures were calculated using the Antoine equation: $\boldsymbol{log(p/Pa)} = \left(\boldsymbol{A} - \frac{\boldsymbol{B}}{\boldsymbol{(T/K+C)}}\right)$.

In general, the vapor pressure data obtained in this work are in good agreement with the literature data [22–28]. Moreover, the ln(*p*) vs. 1/T plot built for both compounds reveals good consistency of the experimental data ($R^2 > 0.99985$).

VLE measurements

In **Figure S2**, the VLE data measured for the ethanol/water mixture (at 13.0 kPa) are compared to the data reported by Beebe et al. [35], at 12.7 kPa, and Voutsas et al. [36], at 13.2 kPa. For comparison purposes, the VLE calculated using the NRTL parameters of the Aspen Plus database was also included in **Figure S2**. All the liquid and vapor phase compositions and the reciprocal temperatures obtained in this work are listed in **Table S4**. The consistency of the VLE results was checked by the thermodynamic consistency test proposed by Kang and co-authors [37]. In this approach, four consistency tests are applied (i.e., Area, van Ness, Point-to-point, and Infinite dilution) to check the quality of the

evaluated dataset. The data obtained for the ethanol/water mixture passed in the Area test, van Ness test, and the Infinite dilution test (quality factor included in **Table S4**). In this work, the non-random two-liquid (NRTL) model [1] with five parameters was applied to represent the VLE of the binary systems. The NRTL parameters for the ethanol/water mixture from the Aspen Plus database and calculated σ deviations between the experimental and calculated data are presented in **Table S5**.

The VLE data obtained for the ethanol/water mixture in this work agree with most of the data reported by Voutsas et al. [36], being the largest differences observed near the azeotropic temperature (1.6 K). In addition, low deviations between the experimental data and predicted with the NRTL model ($\sigma(T) = 0.32$ K and $\sigma(y) = 0.0112$) were obtained. On the other hand, the *T*-*x*-*y* plot built with the data reported by Beebe et al. [35] presents some clear inconsistencies, particularly in the azeotropic region. Beebe and co-authors performed the VLE measurements with a modified Baker still apparatus [38], which is different from the Fisher ebulliometer employed in this work and by Voutsas et al. [36]. Nonetheless, all the *x*-*y* diagrams presented in **Figure S2** show similar trends.

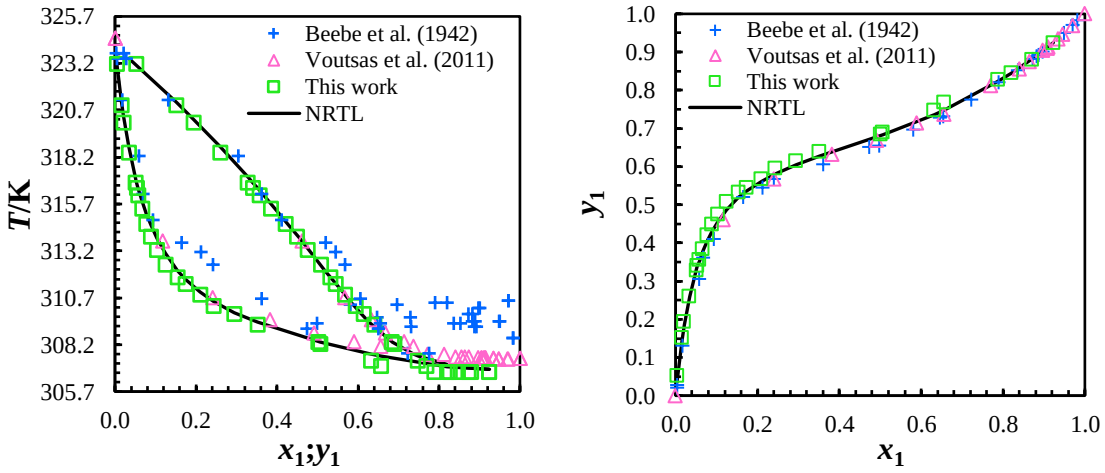

Figure S2. Comparison of the vapor-liquid equilibrium data of the ethanol (1) + water (2) mixture measured in this work and available in the literature [35,36], at 12.9 ± 0.3 kPa.

Table S4. Experimental vapor-liquid equilibrium (VLE) of the ethanol (1) + water (2) binary mixture obtained in this work, at 12.9 ± 0.1 kPa.[a,b]

T/K	x_1	y_1
306.8	0.923	0.923
306.8	0.872	0.879
306.8	0.820	0.846
306.8	0.788	0.827
307.1	0.657	0.768
307.4	0.632	0.747
308.3	0.507	0.690
308.4	0.502	0.684
309.3	0.352	0.640
309.9	0.295	0.614
310.3	0.243	0.595
310.9	0.210	0.568
311.5	0.174	0.544
311.8	0.154	0.532
312.5	0.124	0.508
313.3	0.103	0.475
314.0	0.088	0.448
314.7	0.077	0.421
315.5	0.067	0.384
316.2	0.058	0.357
316.6	0.053	0.340
316.9	0.051	0.328
318.5	0.034	0.260
320.1	0.021	0.194
321.0	0.016	0.152
323.2	0.004	0.052

[a]The estimated uncertainties are u(T) = 0.1 K; u(x) = 0.005; u(y) = 0.005.

[b] Overall quality factor following the methodology proposed by Kang et al [37]: $Q_{VLE} = 0.80$

Table S5. NRTL parameters and obtained root-mean-square deviations (σ) for the VLE data of the binary ethanol (1) + water (2) mixture.

NRTL parameters[a]	
$\boldsymbol{A_{12}}$	-0.80
$\boldsymbol{A_{21}}$	3.46
$\boldsymbol{B_{12}}$	246.18
$\boldsymbol{B_{21}}$	-586.08
$\boldsymbol{\alpha}$	0.3
$\boldsymbol{\sigma}$ *values*	
$\boldsymbol{\sigma(T)/K}$	0.32
$\boldsymbol{\sigma(y_1)}$	0.0112
$\boldsymbol{\sigma(y_2)}$	0.0112

[a]The energy of interactions, G_{ij}, in the NRTL model [1] is calculated as: $G_{ij} = exp\left[-\alpha\left(A_{ij} + \frac{B_{ij}}{T}\right)\right]$; T/K.

Section S4. VLE for binary mixtures

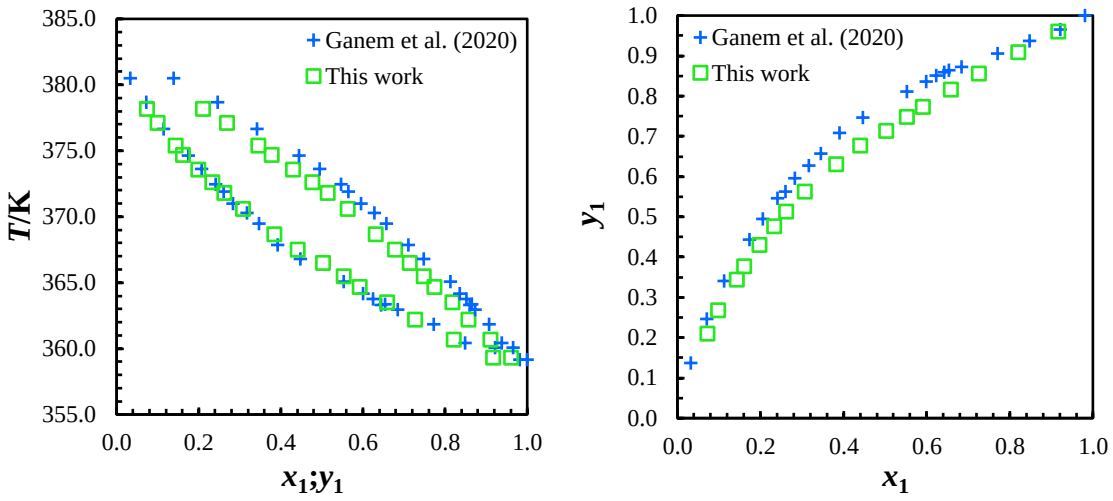

Figure S3. Comparison of the vapor-liquid equilibrium data of the R-(+)-limonene (1) + linalool (2) mixture measured in this work and reported by Ganem et al. [28], at 5.0 ± 0.1 kPa

Section S5. VLE of the ternary systems

Modified McDermott−Ellis consistency test

The McDermott−Ellis consistency test [39] modified by Wisniak and Tamir [40] is a point-to-point test that can identify inconsistency datum in VLE experimental datasets. Briefly, the method implies that two points (a and b) are thermodynamically consistent (i.e., the data pass the test) when the local deviation (D) is lower than the maximum deviation (D_{Max}), which are calculated as follows:

$$D = \sum_{i=1}^{N} [(x_{ia} + x_{ib}) \times (\ln \gamma_{ib} - \ln \gamma_{ia})] \tag{10}$$

$$\begin{aligned} D_{\mathrm{Max}} = & \sum_{i=1}^{N} \left[(x_{ia} + x_{ib}) \times \left(\frac{1}{x_{ia}} + \frac{1}{\gamma_{ia}} + \frac{1}{x_{ia}} + \frac{1}{\gamma_{ib}} \right) \times \Delta x \right] \\ & + 2 \sum_{i=1}^{N} [|\ln \gamma_{ib} - \ln \gamma_{ia}| \times \Delta x] \\ & + \sum_{i=1}^{N} \left[(x_{ia} + x_{ib}) \times \frac{\Delta p}{p} \right] \\ & + \sum_{i=1}^{N} \left\{ (x_{ia} + x_{ib}) \times B_i \times \left[\frac{1}{(T_a + C_i)^2} + \frac{1}{(T_b + C_i)^2} \right] \times \Delta T \right\} \end{aligned} \tag{11}$$

where x_i and γ_i are the liquid phase mole fraction of and the activity coefficients of component i, respectively; N is the total number of components in the mixture; T_a and T_b are the absolute temperature of two datapoints a and b; Δx, Δp and ΔT are the uncertainties in the liquid phase mole fraction, pressure, and temperature, respectively; B_i and C_i are the Antoine constants of component i.

Table S6. Results for the modified McDermott-Ellis test applied to the VLE data obtained in this work for the ternary systems.[a]

R-(+)-limonene (1) + linalool (2) + [C$_4$mim][OAc] (3)				**R-(+)-limonene (1) + linalool (2) + [C$_4$mim]Cl (3)**			
$x_{a,1}$-$x_{b,1}$	$\|D\|$	D_{max}	*Result*	$x_{a,1}$-$x_{b,1}$	$\|D\|$	D_{max}	*Result*
0.885-0.824	0.021	0.148	Pass	0.691-0.651	0.003	0.151	Pass
0.824-0.773	0.022	0.145	Pass	0.651-0.619	0.004	0.150	Pass
0.773-0.715	0.006	0.145	Pass	0.619-0.575	0.007	0.149	Pass
0.715-0.659	0.016	0.144	Pass	0.575-0.549	0.008	0.148	Pass
0.659-0.610	0.004	0.142	Pass	0.549-0.530	0.009	0.147	Pass
0.610-0.554	0.009	0.140	Pass	0.530-0.474	0.002	0.146	Pass
0.554-0.495	0.015	0.138	Pass	0.474-0.439	0.002	0.143	Pass
0.495-0.449	0.006	0.136	Pass	0.439-0.401	0.007	0.140	Pass
0.449-0.400	0.013	0.133	Pass	0.401-0.369	0.002	0.138	Pass
0.400-0.353	0.004	0.131	Pass	0.369-0.334	0.007	0.136	Pass
0.353-0.314	0.015	0.130	Pass	0.334-0.292	0.011	0.134	Pass
0.314-0.279	0.003	0.128	Pass	0.292-0.256	0.019	0.131	Pass
0.279-0.241	0.004	0.126	Pass	0.256-0.224	0.008	0.129	Pass
0.241-0.202	0.005	0.124	Pass	0.224-0.192	0.015	0.127	Pass
0.202-0.175	0.009	0.122	Pass	0.192-0.168	0.006	0.125	Pass
0.175-0.156	0.006	0.120	Pass	0.168-0.149	0.005	0.123	Pass
0.156-0.143	0.005	0.119	Pass	0.149-0.137	0.003	0.122	Pass
0.143-0.117	0.007	0.119	Pass	0.137-0.126	0.004	0.121	Pass
0.117-0.103	0.005	0.117	Pass	0.126-0.114	0.004	0.120	Pass
0.103-0.085	0.004	0.116	Pass	0.114-0.092	0.000	0.119	Pass
0.085-0.071	0.005	0.115	Pass	0.092-0.072	0.017	0.118	Pass
0.071-0.030	0.009	0.119	Pass	0.072-0.058	0.024	0.116	Pass
				0.058-0.041	0.038	0.115	Pass
				0.041-0.025	0.057	0.114	Pass

[a] $\Delta x = 0.005$; $\Delta p = 0.1\ kPa$; $\Delta T = 0.1\ K$.

Relative volatility

The relative volatility of a mixture of two compounds is calculated as follows:

$$\alpha_{12} = \frac{{y_1}/{x_1'}}{{y_2}/{x_2'}} \quad \textbf{(S1)}$$

where y_i is the mole fraction of compound *i* in the vapor phase, x'_i is its mole fraction in the liquid phase (on an IL-free basis), and the subscripts 1 and 2 correspond to R-(+)-limonene and linalool, respectively.

Section S6. Process simulation complementary information

Table S7. List of the correlated NRTL parameters and obtained root-mean-square deviations (σ) for the VLE data of limonene/linalool and limonene/linalool/IL mixtures.

	Limonene (1) + linalool (2)	**Limonene (1) + linalool (2) + [C_4mim][OAc] (3)**	**Limonene (1) + linalool (2) + [C_4mim]Cl (3)**
	NRTL Parameters[a]		
$\boldsymbol{A_{12}}$	-11.43	-13.38	-20.08
$\boldsymbol{A_{21}}$	-1.45	3.32	24.53
$\boldsymbol{B_{12}}$	3787.60	4496.94	7019.89
$\boldsymbol{B_{21}}$	1572.53	-168.67	-8164.34
$\boldsymbol{A_{13}}$		-336.19	-7.39
$\boldsymbol{A_{31}}$		73.77	19.05
$\boldsymbol{B_{13}}$		291879.16	-10403.89
$\boldsymbol{B_{31}}$		24057.16	-5068.65
$\boldsymbol{A_{23}}$		86.12	-60.30
$\boldsymbol{A_{32}}$		7.72	4.71
$\boldsymbol{B_{23}}$		82954.60	10559.09
$\boldsymbol{B_{32}}$		-3147.20	-3001.49
$\boldsymbol{\alpha}$	0.3	0.3	0.3
	σ *values*		
$\boldsymbol{\sigma(T)/\mathrm{K}}$	0.71	0.15	0.06
$\boldsymbol{\sigma(p)/\mathrm{kPa}}$	0.009	0.002	0.001
$\boldsymbol{\sigma(x_1)}$	0.0003	0.0001	0.0001
$\boldsymbol{\sigma(x_2)}$	0.0003	0.0001	0.0197
$\boldsymbol{\sigma(y_1)}$	0.0068	0.0208	0.0040
$\boldsymbol{\sigma(y_2)}$	0.0064	0.0246	0.0052

[a]The energy of interactions, G_{ij}, in the NRTL model [1] is calculated as: $G_{ij} = exp\left[-\alpha\left(A_{ij} + \frac{B_{ij}}{T}\right)\right]$; *T*/K.

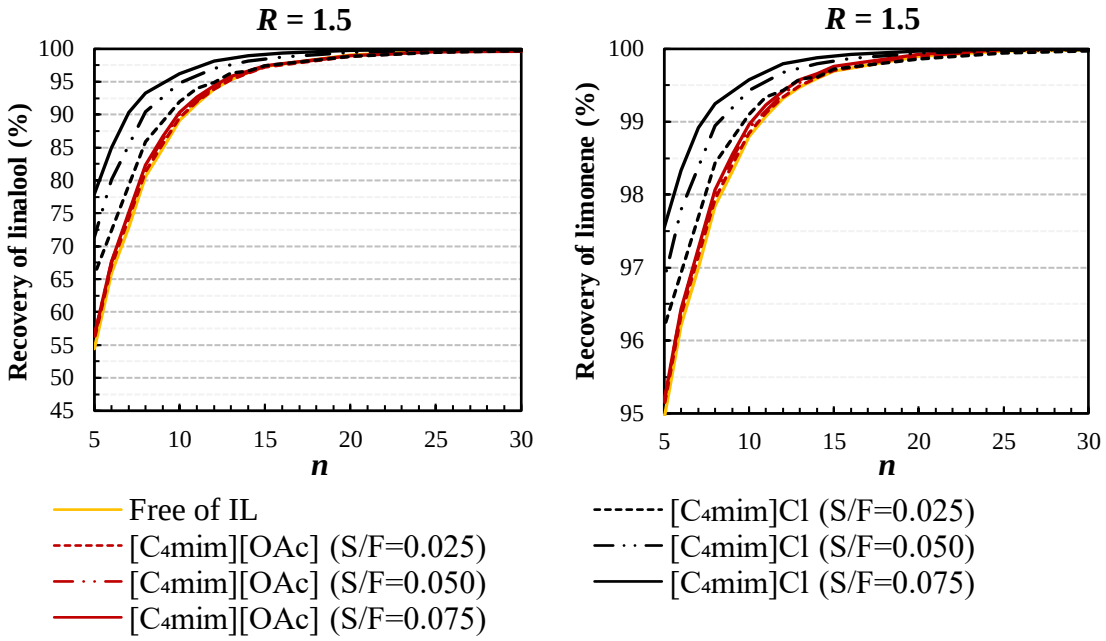

Figure S4. Comparison of the limonene and linalool recoveries (%) as function of the number of stages in the distillation column for R = 1.5 and different S/F ratios.

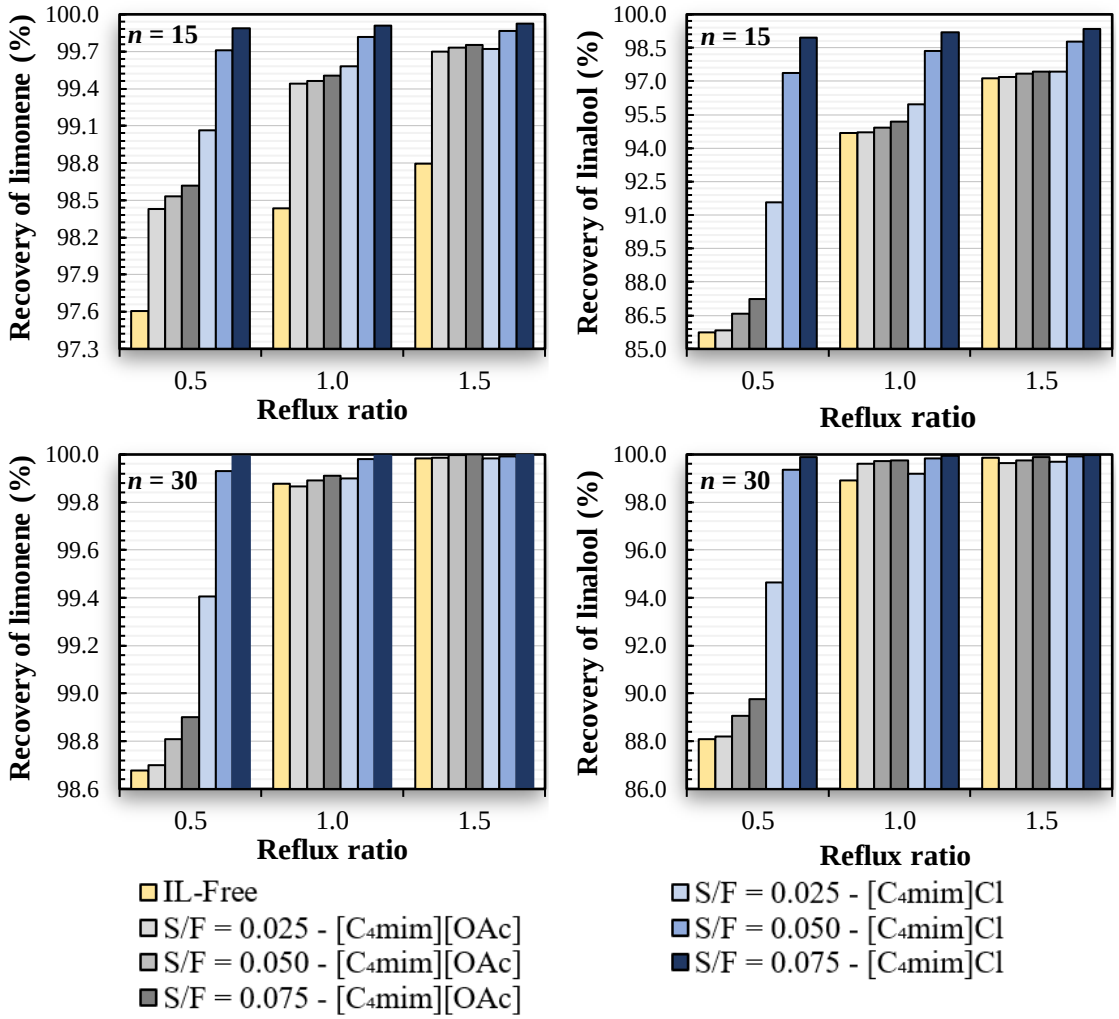

Figure S5. Overview of recoveries of limonene and linalool obtained for different S/F and R values, fixing $n = 15$ and $n = 3$.

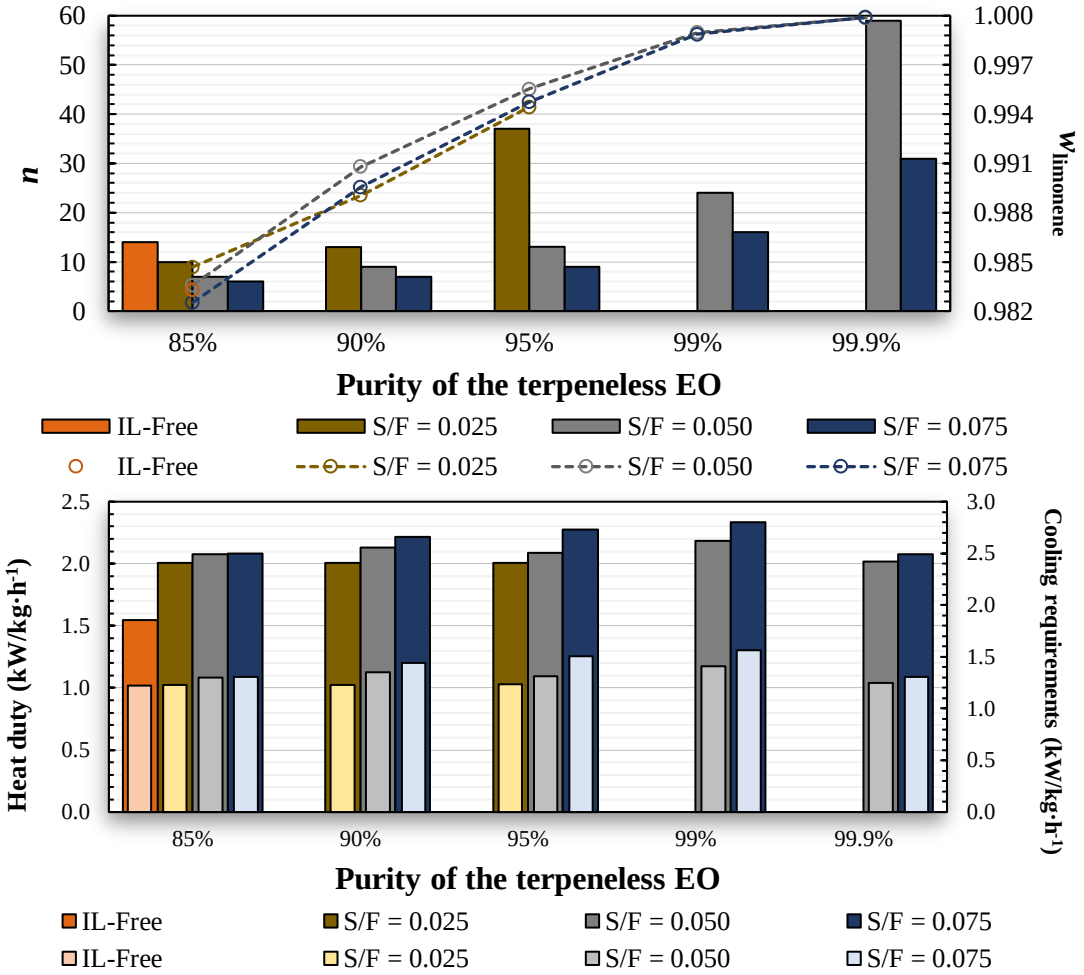

Figure S6. Overview of the requirements to obtain the target linalool purities in the terpeneless CEO from the process free of IL and with [C4mim]Cl, for $R = 0.5$. The dark bars correspond to n or the specific heat duty, the light bars are the specific cooling requirements, and the circles represent the limonene mass fraction obtained in the distillate. The lines connecting the circles are guides for the eyes.

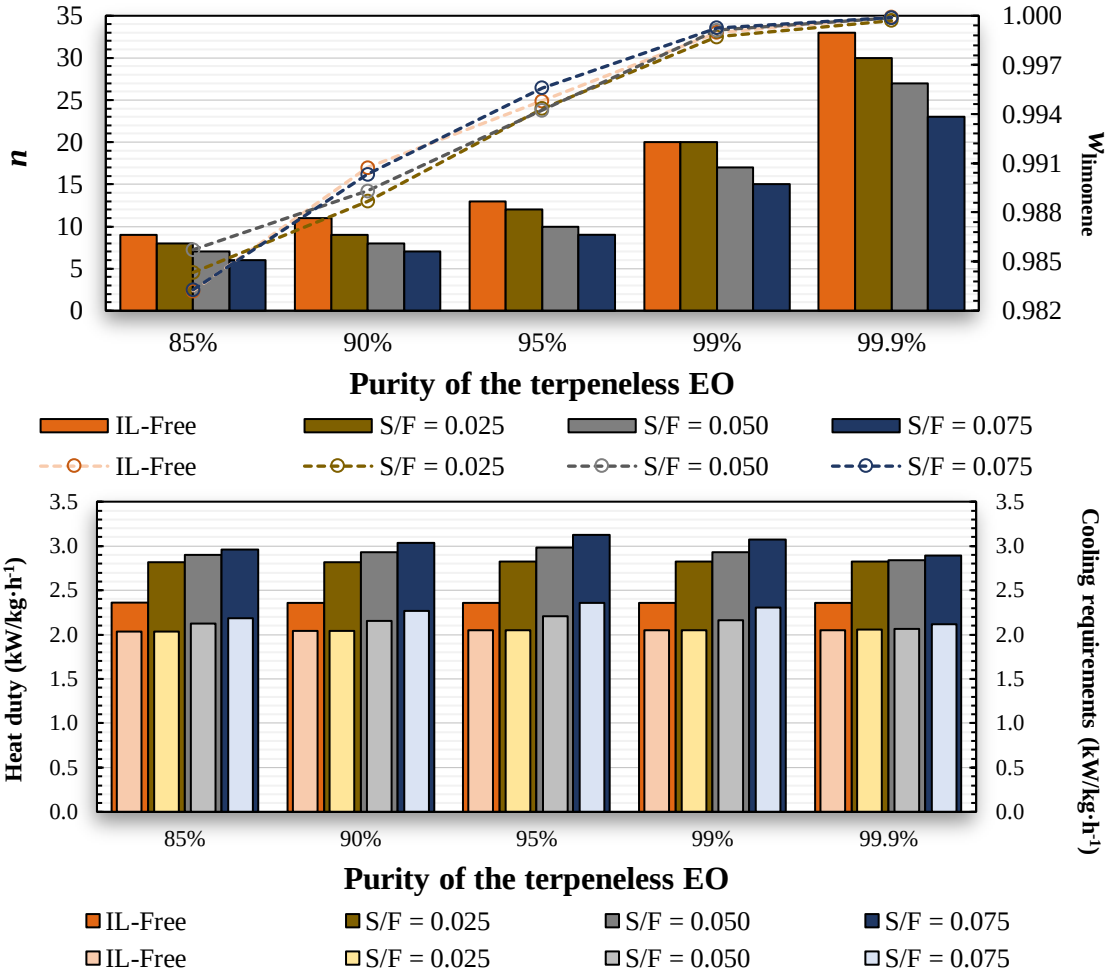

Figure S7. Overview of the requirements to obtain the target linalool purities in the terpeneless CEO from the process free of IL and [C4mim]Cl, for $R = 1.5$. The dark bars correspond to n or the specific heat duty, the light bars are the specific cooling requirements, and the circles represent the limonene mass fraction obtained in the distillate. The lines connecting the circles are guides for the eyes.

References

[1] Renon H, Prausnitz JM. Local compositions in thermodynamic excess functions for liquid mixtures. AIChE J 1968;14:135–44.

[2] Qin Y, Chen X, Wang L, Wei X, Mo H, Wei X, et al. Measurement and correlation of isothermal vapor-liquid equilibrium for (−)-β-caryophyllene + p-cymene with dehydroabietic acid at 313.15, 323.15, and 333.15K. J Taiwan Inst Chem Eng 2022;138:104466.

[3] Turek C, Stintzing FC. Stability of essential oils: A review. Compr Rev Food Sci Food Saf 2013;12:40–53.

[4] Gutiérrez-Guerra R, Segovia-Hernández JG, Hernández S. Reducing energy consumption and CO2 emissions in extractive distillation. Chem Eng Res Des 2009;87:145–52.

[5] Li G, Liu S, Yu G, Dai C, Lei Z. Extractive distillation using ionic liquids-based mixed solvents combined with dividing wall column. Sep Purif Technol 2021;269:118713.

[6] Gadalla MA, Olujic Z, Jansens PJ, Jobson M, Smith R. Reducing CO2 emissions and energy consumption of heat-integrated distillation systems. Environ Sci Technol 2005;39:6860–70.

[7] Gao X, Yang Y, Chen M, Cheng Q, Lu K. Novel heat pump reactive distillation and dividing-wall column reactive distillation processes for synthesizing isopropyl acetate to save TAC and reduce CO2 emissions. Chem Eng Process - Process Intensif 2022;171:108746.

[8] Zhu Z, Hu J, Geng X, Qin B, Ma K, Wang Y, et al. Process design of carbon dioxide and ethane separation using ionic liquid by extractive distillation. J Chem Technol Biotechnol 2018;93:887–96.

[9] Yang B, Cheng Y, Chen K, Wei Z, Lei Z, Li G. Ester hydrolysis to alcohol using a combined reactive and extractive distillation with ionic liquids-based mixed solvents. Fuel 2022;327:125131.

[10] Hekayati J, Roosta A, Javanmardi J. On the prediction of the vapor pressure of ionic liquids based on the principle of corresponding states. J Mol Liq 2017;225:118–26.

[11] Valderrama JO, Sanga WW, Lazzús JA. Critical properties, normal boiling temperature, and acentric factor of another 200 ionic liquids. Ind Eng Chem Res

2008;47:1318–30.

[12] Strechan AA, Paulechka YU, Blokhin AV, Kabo GJ. Low-temperature heat capacity of hydrophilic ionic liquids [BMIM][CF3COO] and [BMIM][CH3COO] and a correlation scheme for estimation of heat capacity of ionic liquids. J Chem Thermodyn 2008;40:632–9.

[13] Holbrey JD, Reichert WM, Nieuwenhuyzen M, Johnson S, Seddon KR, Rogers RD. Crystal polymorphism in 1-butyl-3-methylimidazolium halides: supporting ionic liquid formation by inhibition of crystallization. Chem Commun 2003;3:1636–7.

[14] Ge R, Hardacre C, Jacquemin J, Nancarrow P, Rooney DW. Heat capacities of ionic liquids as a function of temperature at 0.1 MPa. Measurement and prediction. J Chem Eng Data 2008;53:2148–53.

[15] Moldover MR, Trusler JPM, Edwards TJ, Mehl JB, Davis RS. Measurement of the Universal Gas Constant R Using a Spherical Acoustic Resonator. Phys Rev Lett 1988;60:249–52.

[16] Verevkin SP, Zaitsau DH, Ludwig R. Aprotic ionic liquids: A framework for predicting vaporization thermodynamics. Molecules 2022;27:2321.

[17] Pence HE, Williams A. Chemspider: An online chemical information resource. J Chem Educ 2010;87:1123–4.

[18] ChemSpider. R Soc Chem 2021. https://www.chemspider.com/ (accessed December 8, 2021).

[19] Wei J, Bu X, Guan W, Xing N, Fang D, Wu Y. Measurement of vaporization enthalpy by isothermogravimetrical method and prediction of the polarity for 1-alkyl-3-methylimidazolium acetate {[C n mim][OAc] (n = 4, 6)} ionic liquids. RSC Adv 2015;5:70333–8.

[20] Verevkin SP, Zaitsau DH, Emel'yanenko VN, Schick C, Jayaraman S, Maginn EJ. An elegant access to formation and vaporization enthalpies of ionic liquids by indirect DSC experiment and "in silico" calculations. Chem Commun 2012;48:6915.

[21] Linstrom PJ, Mallard WG, editors. NIST Chemistry WebBook, NIST Standard Reference Database Number 69. Gaithersburg MD: National Institute of Standards and Technology; 2022.

[22] Ambrose D, Sprake CHS. Thermodynamic properties of organic oxygen compounds XXV. Vapour pressures and normal boiling temperatures of aliphatic

alcohols. J Chem Thermodyn 1970;2:631–45.

[23] Steele W V., Chirico RD, Cowell AB, Knipmeyer SE, Nguyen A. Thermodynamic properties and ideal-gas enthalpies of formation for methyl benzoate, ethyl benzoate, (R)-(+)-limonene, tert-amyl methyl ether, trans-crotonaldehyde, and diethylene glycol. J Chem Eng Data 2002;47:667–88.

[24] Ngema PT, Matkowska D, Naidoo P, Hofman T, Ramjugernath D. Vapor-liquid equilibrium data for binary systems of 1-methyl-4-(1- methylethenyl)-cyclohexene + {ethanol, propan-1-ol, propan-2-ol, butan-1-ol, pentan-1-ol, or hexan-1-ol} at 40 kPa. J Chem Eng Data 2012;57:2053–8.

[25] Guetachew T, Mokbel I, Batiu I, Cisse Z, Jose J. Vapor pressures and sublimation pressures of eight constituets of essential oils at pressures in the range from 0.3 to 83,000 Pa. ELDATA Int Eletronic J Physico-Chemical Data 1999;5:43–53.

[26] Batiu I, Esteller LJ. Vapor liquid equilibria in binary systems (+)-carvone + (+)-limonene at temperatures between 365 and 411 K. ELDATA Int Eletronic J Physico-Chemical Data 1996;2:59–66.

[27] Espinosa Díaz MA, Guetachew T, Landy P, Jose J, Voilley A. Experimental and estimated saturated vapour pressures of aroma compounds. Fluid Phase Equilib 1999;157:257–70.

[28] Ganem F, Mattedi S, Rodríguez O, Rodil E, Soto A. Deterpenation of citrus essential oil with 1-ethyl-3-methylimidazolium acetate: A comparison of unit operations. Sep Purif Technol 2020;250:117208.

[29] Kretschmer CB, Wiebe R. Liquid-vapor equilibrium of ethanol-toluene solutions. J Am Chem Soc 1949;71:1793–7.

[30] Kojima K, Kato M. Measurements of isobaric boiling point curves at high and low pressures. Chem Eng 1969;33:769–75.

[31] Perbemton RC, Mash CJ. Thermodynamic properties of aqueous non-electrolyte mixtures II. Vapour pressures and excess Gibbs energies for water + ethanol at 303.15 to 363.15 K determined by an accurate static method. J Chem Thermodyn 1978;10:867–88.

[32] Muthu OI, Maher PJ, Smith BD. Vapor-liquid equilibrium for the binary systems propionitrile + ethylbenzene and acetonitrile + ethyl acetate, + ethyl alcohol, and + toluene. J Chem Eng Data 1980;25:163–70.

[33] Mousa AHN. Critical properties, heat of vaporization and vapour pressure of ethanol from 20kPa to the critical point. J Chem Eng Japan 1987;20:635–7.

[34] Oktavian R, Amidelsi V, Rasmito A, Wibawa G. Vapor pressure measurements of ethanol-isooctane and 1-butanol-isooctane systems using a new ebulliometer. Fuel 2013;107:47–51.

[35] Beebe AH, Coulter KE, Lindsay RA, Baker EM. Equilibria in ethanol-water system at pressures less than atmospheric. Ind Eng Chem 1942;34:1501–4.

[36] Voutsas EC, Pamouktsis C, Argyris D, Pappa GD. Measurements and thermodynamic modeling of the ethanol-water system with emphasis to the azeotropic region. Fluid Phase Equilib 2011;308:135–41.

[37] Kang JW, Diky V, Chirico RD, Magee JW, Muzny CD, Abdulagatov I, et al. Quality assessment algorithm for vapor-liquid equilibrium data. J Chem Eng Data 2010;55:3631–40.

[38] Coulter KE, Lindsay RA, Baker EM. The system aniline-chlorobenzene. Ind Eng Chem 1941;33:1251–3.

[39] McDermott C, Ellis SRM. A multicomponent consistency test. Chem Eng Sci 1965;20:293–6.

[40] Wisniak J, Tamir A. Vapor-liquid equilibriums in the ternary systems water-formic acid-acetic acid and water-acetic acid-propionic acid. J Chem Eng Data 1977;22:253–60.